the layered material under discussion (in comparison with the classical problem). The group velocity increases from zero (at the blocking frequency) to the largest values at frequencies at which $c_m < c < c_f$, and it also tends to $c_m$ as $\omega \to \infty$.

LITERATURE CITED


1. M. O. Shul'ga and V. G. Savin, "Love waves in a layered composite," Dop. Akad. Nauk Ukr. RSR, Ser. A, No. 10, 926-928 (1973).
2. V. G. Savin and N. A. Shul'ga, "Phase and group velocities of a Love surface wave in a layered medium," Akust. Zh., 21, No. 2, 260-263 (1975).
3. N. A. Shul'ga, Principles of the Mechanics of Layered Media of Periodic Structure [in Russian], Kiev (1981).
4. A. K. Malmeister, V. P. Tamuzh, and G. A. Teters, The Strength of Polymeric and Composite Materials [in Russian], 3rd ed., Riga (1980).
5. V. M. Antonenko, A. N. Podlipenets, and N. A. Shul'ga, "The propagation of body shear waves in orthotropic layered composites," Mekh. Kompozitn. Mater., No. 1, 145-149 (1982).
6. L. M. Brekhovskikh, Waves in Layered Media, Academic Press (1960).


# PREDICTING THE CREEP OF UNIDIRECTIONAL REINFORCED PLASTIC WITH THERMORHEOLOGICALLY SIMPLE STRUCTURAL COMPONENTS


R. D. Maksimov and É. Z. Plume



UDC 539.376:678.067.5


In investigating the thermoelastic properties of fibrous polymer composites, many studies have established observance of the temperature–time analogy and demonstrated on this basis the possibility of predicting the long-term rheologic resistance of these materials from the results of accelerated tests. Thus, observance of the analogy is demonstrated for various fiberglasses in [1-6] and in studying the relaxation properties of fiberglasses in [7], while observance of the analogy for high-strength organoplastic is exposed in [8]. In the majority of cases, the composite is treated as a quasihomogeneous anisotropic material; as a rule, the question concerning a relationship between the temperature–shear function and the volume content and orientation of reinforcing fibers has not been studied. Strictly speaking, the data used for this prediction therefore characterize the properties of the tested components alone, and could not be used in optimization problems for the structure of reinforcement with allowance for the long-term deformation properties of the structural components.

Our objective in this study was to investigate the possibility of the staged prediction of the viscoelastic properties of a composite, the structural components of which can be considered thermorheologically simple bodies: first to perform accelerated tests on the components and to predict their viscoelastic properties, and then, using prediction data and structural models, to determine by computational means the long-term viscoelastic properties of the composite with allowance for the structure of the reinforcement. This approach is more fundamental in cases where a composite material consisting of thermorheologically simple components develops a thermorheologically complex behavior; this may be caused not only by processes at the fiber/binder interface, but also by the formation of boundary layers. This is easy to demonstrate as an example on the simplest model of a unidirectional composite. We will assume that in such a fiber/matrix composite there are viscoelastic thermorheologically simple materials whose rheological properties in the linear strain region are described in accordance with Boltzmann–Volterra hereditary theory using the reciprocal equations

$$\varepsilon(t)=\frac{1}{F}\left[\sigma(t)+\int_0^t K(t-s,T)\sigma(s)\,ds\right];$$
$$\sigma(t)=E\left[\varepsilon(t)-\int_0^t R(t-s,T)\varepsilon(s)\,ds\right], \qquad (1)$$


Institute of Polymer Mechanics, Academy of Sciences of the Latvian SSR, Riga.


Translated from Mekhanika Kompozitnykh Materialov, No. 6, pp. 1081-1089, November-December, 1982. Original article submitted May 17, 1982.

where σ is stress, ε is strain, E is the elastic modulus, K and R are creep and relaxation kernels, t is time, and T is temperature. In the isothermal case, the K and R kernels depend on temperature as a parameter. Analytical expressions for the kernels can be adopted in the form of the sum of the exponents

$$K(t-s,T)=\sum_{i=1}^{k}A_i(T)\alpha_i(T)e^{-\alpha_i(T)(t-s)};$$
$$R(t-s,T)=\sum_{i=1}^{k}B_i(T)\beta_i(T)e^{-\beta_i(T)(t-s)}. \tag{2}$$

The temperature–time analogy will apply only when the following conditions are observed:

$$A_i=\text{inv}(T);\quad \alpha_i(T)=\alpha_i^0 a_T;\quad \alpha_i^0=\text{inv}(T);$$
$$B_i=\text{inv}(T);\quad \beta_i(T)=\beta_i^0 a_T;\quad \beta_i^0=\text{inv}(T), \tag{3}$$

where $a_T$ is a temperature–shear function. Substitution of equality (3) in (2) and introduction of conditional time t' and s' from the equations t' = $a_T$t and s' = $a_T$s reduce Eq. (1) to a temperature-invariant form (with coefficients independent of temperature). If it is assumed that in loading the composite in the direction of the reinforcement, the fibers and binder are in a uniaxial stressed state and temperature stresses are neglected, the relation between the stress–strain state of the composite and its components will be determined by the following system of equations:

$$\sigma_a(t)=E_a\left[\varepsilon(t)-\int_0^t R_a(t-s,T)\varepsilon(s)\,ds\right];$$
$$\sigma_m(t)=E_m\left[\varepsilon(t)-\int_0^t R_m(t-s,T)\varepsilon(s)\,ds\right]; \tag{4}$$
$$\mu\sigma_a(t)+(1-\mu)\sigma_m(t)=\sigma,$$

where ε(t) is the deformation of the composite under a constant stress σ, and μ is the reinforcing factor; the subscript $a$ pertains to fiber characteristics, and the subscript m to binder characteristics. After certain transformations, we can reduce system (4) to the second-order Volterra integral equation

$$\frac{\sigma}{\mu E_a+(1-\mu)E_m}=\varepsilon(t)-\int_0^t\left[\frac{\mu E_a}{\mu E_a+(1-\mu)E_m}R_a(t-s,T)+\frac{(1-\mu)E_m}{\mu E_a+(1-\mu)E_m}R_m(t-s,T)\right]\varepsilon(s)\,ds. \tag{5}$$

The solution of Eq. (5) can be represented in the following form:

$$\varepsilon(t)=\frac{\sigma}{\mu E_a+(1-\mu)E_m}\left[1+\int_0^t\Gamma(t-s,T)\,ds\right], \tag{6}$$

where Γ(t − s, T) is the resolvent of the kernel

$$R(t-s,T)=\frac{\mu E_a}{\mu E_a+(1-\mu)E_m}R_a(t-s,T)+\frac{(1-\mu)E_m}{\mu E_a+(1-\mu)E_m}R_m(t-s,T). \tag{7}$$

Creep testing is normally a method more widely used for experimental determination of the parameters of hereditary kernels; it will therefore be required to determine the relaxation kernels $R_\alpha$ and $R_m$ that enter into (7) from the creep kernels $K_\alpha$ and $K_m$. Making use of (2) and considering (3), we can write analytical expressions of the kernels for the fiber:

$$K_a(t-s,T)=\sum_{i=1}^{k}A_{ia}\alpha_{ia}{}^0a_{Ta}\exp[-\alpha_{ia}{}^0a_{Ta}(t-s)];$$

$$R_a(t-s, T) = \sum_{i=1}^{k} B_{ia}\beta_{ia}{}^0 a_{Ta} \exp[-\beta_{ia}{}^0 a_{Ta}(t-s)].$$

The dependence of $K_\alpha$ and $R_\alpha$ on T as a parameter in the case T = const under consideration does not change the familiar [9] relationships relating the parameters of the kernel and resolvent. Therefore, $\beta_{i\alpha}^0$ are determined as k real and positive roots of the k-th-order polynomial

$$\sum_{i=1}^{k} \frac{A_{ia}\alpha_{ia}{}^0}{\beta_a{}^0 - \alpha_{ia}{}^0} = 1;$$

the roots of the polynomial are located between bands, i.e., $\alpha_{l\alpha}{}^0 < \beta_{l\alpha}{}^0 < \alpha_{l+1,\alpha}{}^0$, $\alpha_{k\alpha}{}^0 < \beta_{k\alpha}{}^0$ [10] and can be determined by the iteration method. Since one and only one root $\beta_{l\alpha}{}^0$ exists for each section $[\alpha_{l\alpha}{}^0, \alpha_{l+1,\alpha}{}^0]$, it can be rather easily determined by successive division of the section into two equal parts $[\alpha_{l\alpha}{}^0, \alpha_{l+1,\alpha}{}^0]$ [11]. Unknowns $B_{i\alpha}$ are determined by solution of the following linear algebraic system [9]:

$$\sum_{i=1}^{k} \frac{B_{ia}\beta_{ia}{}^0}{\beta_{ia}{}^0 - \alpha_{ja}{}^0} = 1 \quad (j = 1, \ldots, k).$$

Analytical expressions of the hereditary kernels for the binder can also be adopted as the sum of the exponents

$$K_m(t-s, T) = \sum_{i=1}^{n} A_{im}\alpha_{im}{}^0 a_{Tm} \exp[-\alpha_{im}{}^0 a_{Tm}(t-s)];$$

$$R_m(t-s, T) = \sum_{i=1}^{n} B_{im}\beta_{im}{}^0 a_{Tm} \exp[-\beta_{im}{}^0 a_{Tm}(t-s)].$$

The unknowns $B_{im}$ and $\beta_{im}{}^0$ are determined by the method outlined above.

Thus, the parameters entering into (7) are determined. Let us now adopt an analytical expression $\Gamma(t)$ as the sum k + n of the exponents

$$\Gamma(t) = \sum_{i=1}^{k+n} \gamma_i C_i e^{-\gamma_i t}. \tag{8}$$

Instead of (6), we then arrive at the following relationship for the creep of a unidirectional composite in the direction of the reinforcement:

$$\varepsilon(t) = \frac{\sigma}{\mu E_a + (1-\mu)E_m}\left[1 + \sum_{i=1}^{k+n} C_i(1 - e^{-\gamma_i t})\right]. \tag{9}$$

The $\Gamma(t)$ function is the resolvent in terms of the R(t) kernel; according to equations describing the relation beween the parameters of the kernel and resolvent, the unknowns $C_i$ and $\gamma_i$ can therefore be determined from (7) with consideration of (8); the methods of derivation are similar to those outlined above for determination of the parameters of the fiber and binder kernels. In this case, it is easily seen that $C_i$ and $\gamma_i$ depend on $E_\alpha$, $E_m$, $\mu$, $A_{i\alpha}$, $A_{im}$, $\alpha_{i\alpha}$, $\alpha_{im}$, $a_{T\alpha}$, $a_{Tm}$. Thus, if the structural components of a reinforced plastic are thermorheologically simple materials, yet the temperature–shear functions of the fiber $a_{T\alpha}$ and binder $a_{Tm}$ are equal, the temperature dependence of the viscoelastic properties of the plastic cannot be expressed using the single function $a_T$, and, consequently, the composite is a thermorheologically complex material. Note, however, that the reinforcement of plastic with viscoelastic fibers with a significantly lower flexibility as compared with the binder suppresses to a large degree (especially for the direction of the reinforcement) the effect of the $a_{Tm}$ function on the temperature dependence of the flexibility of the composite itself; observance of the temperature–time analogy is therefore determined not only by the extent of the difference between $a_{T\alpha}$ and $a_{Tm}$, but also to a considerable degree by the relationship between the flexibility of the structural components and the magnitude of the reinforcing factor. This problem will be discussed in greater detail below as an example of the experimental data obtained in the study.

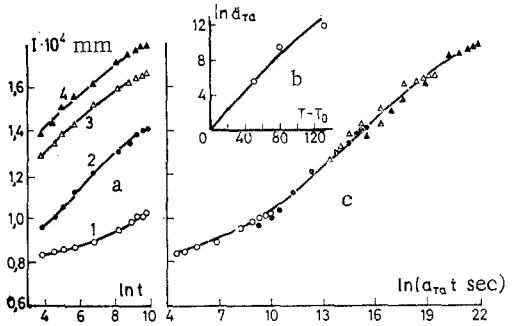


Fig. 1

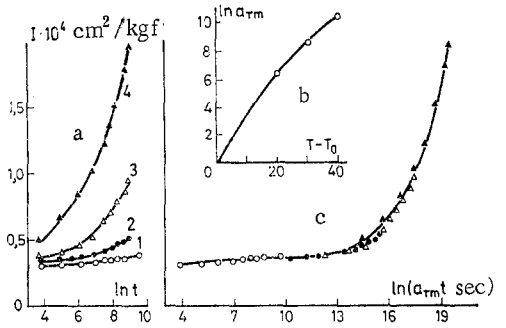


Fig. 2

Fig. 1. Yield curves of organic fiber: a) initial curves at temperature of 20 (1), 70 (2), 100 (3), and 150°C (4); b) temperature–shear function at $T_0$ = 20°C; c) generalized yield curve reduced to $T_0$ = 20°C.

Fig. 2. Yield curves of solidified EDP-10 binder: a) initial curves at 20 (1), 40 (2), 50 (3), and 60°C (4); b) temperature–shear function at $T_0$ = 20°C; c) generalized yield curve reduced to $T_0$ = 20°C.

If the equality $a_{T\alpha} = a_{Tm} = a_T$ exists, Eq. (9) can be represented in the following form:

$$\varepsilon(t) = \frac{\sigma}{\mu E_a + (1-\mu)E_m}\left[1 + \sum_{i=1}^{k+n} C'_i(1 - e^{-a_T \gamma'_i t})\right].$$

Here, $C'_i = \mathrm{inv}(T)$, $\gamma'_i = \mathrm{inv}(T)$, the temperature effect is taken into account using the single function $a_T$, and the rheological properties of the composite can be considered thermorheologically simple.

Let us now assume that the reinforcing fibers are elastic, and the binder a thermorheologically simple material with the temperature-shear function $a_{Tm} = a_T$. In system of Eqs. (4), the first integral equation is then replaced by the algebraic equation $\sigma_\alpha(t) = E_\alpha \varepsilon(t)$, and the solution for $\varepsilon(t)$ will be

$$\varepsilon(t) = \frac{\sigma}{\mu E_a + (1-\mu)E_m}\left[1 + \sum_{i=1}^{n} C''_i(1 - e^{-a_T \gamma''_i t})\right]$$

where $C''_i$ and $\gamma''_i$ are independent of temperature. Consequently, the temperature–time analogy is also observed in this case for the reinforced plastic.

Let us now examine the results of experimental confirmation of the possibility of predicting the long-term creep of a composite from the properties of structural components as determined from accelerated tests. It is known [12-14] that these composites being distinguished by relatively high specific strength indicators, develop increased creep under prolonged loading, even in the direction of the reinforcement.

We subjected specimens of fiber, binder, and a unidirectional reinforced composite based on them to creep tests. Specimens of solidified binder were prepared from a grade EDT-10 epoxy binder. Fiber specimens were clusters of organic fibers impregnated with binder with subsequent solidification under temperature–time conditions similar to the solidification conditions used for organoplastic blanks; this fiber treatment was carried out to reduce the difference in the properties of the fiber specimens and the properties of the fibers in the composite, since in first approximation, we can assume that the effects of physicochemical interaction between the binder and fiber on the whole manifest themselves similarly during the heat treatment of organoplastic blanks and specimens of a fiber cluster impregnated with binder.

The fiber, binder, and organoplastic specimens were tested for short-term (up to 5 h) creep with $\sigma$ = const at several temperature levels, and for long-term (5 yr) creep at $T \approx 20$°C. The results cited below apply to stress ranges in which the assumption concerning the observance of linearity in thermoviscoelastic properties can be made for the materials investigated; the region of linearity is evaluated by the method described in [15] with allowance for temperature effects.

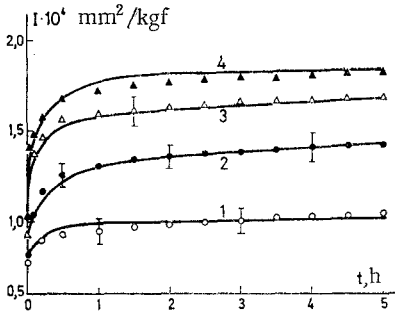


Fig. 3

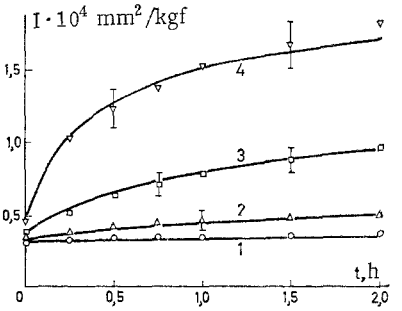


Fig. 4

Fig. 3. Yield curves for organic fiber at T = 20 (1), 70 (2), 100 (3), and 150°C (4). Points indicate average experimental data; lines denote approximation from Eq. (10).

Fig. 4. Yield curves for solidified binder at T = 20 (1), 40 (2), 50 (3), and 60°C (4). Points indicate average experimental data; lines denote approximation from Eq. (10).

Let us first examine the test results of the fiber and binder specimens. A series of averaged yield I(ln t, T) curves of the organic fiber and binder, which were obtained from short-term-creep tests at $\sigma$ = const and four temperature levels, are shown in Figs. 1a and 2a. It is known that preliminary confirmation of observance of the temperature–time analogy consists in determining the displacements of the I(ln t, T) curves along the ln t axis and evaluating the possibility of constructing a generalized curve on the conventional time scale I(ln t'). This analysis was conducted using an algorithm realized in the form of a computer program [16]; the essence of this algorithm consists in a preliminary description of the experimental I(ln t, T) curves by a polynomial of the required order in accordance with the least-squares method, determination of logarithmic shear, description of the $a_T$ function, and delivery of the final result of the computation – a generalized yield curve given in the form of a table and reduced to the base temperature $T_0$. A graphic illustration of the results of the analysis is presented in Figs. 1 and 2. The resultant ln $a_{T\alpha}$ and ln $a_{Tm}$ values are described well by the familiar Williams–Landell–Ferry equation

$$\ln a_T = \frac{c_1(T-T_0)}{c_2+(T-T_0)}$$

for the following values of the coefficients: $c_1$ = 70.7 and $c_2$ = 582 for the fibers, and $c_1$ = 25.8 and $c_2$ = 59.9 for the binder (see Fig. 1b and 2b); note that the same base-temperature value $T_0$ = 20°C is adopted for the fiber and binder. The generalized yield curves obtained by reduction to $T_0$ = 20°C are presented in Figs. 1c and 2c. The possibility of the generalization of the I(ln t, T) curves suggests that they differ only in time scale, i.e., I(ln t, T) = I(ln t + ln $a_T$) = I [ln($a_T$t)] = I(ln t'). Consequently, short-term-creep curves obtained for $\sigma$ = const at different temperatures may be described by the expression

$$\varepsilon(t) = \sigma\left\{a + b\frac{1}{k}\sum_{i=1}^{k}\left[1-\exp\left(-ta_T/\tau_{0i}\right)\right]\right\}, \qquad (10)$$

where $\tau_{0i}$ is the spectrum of relaxation times at the base temperature $T_0$.

The parameters entering into (10) are determined via computer using the algorithm in [17], on the basis of which a modification of the method of most rapid descent is proposed. The purpose function is adopted in the following form

$$\Phi = \frac{1}{MN}\sum_{m=1}^{M}\sum_{n=1}^{N}\left[\left(\varepsilon_{mn}^{e}-\varepsilon_{m}^{c}\right)/\varepsilon_{m}^{e}\right]^2 \to \min,$$

where the superscripts "e" and "c" denote, respectively, the experimental and computed strain values, N is the number of concurrent tests for each level of T, and M is the total number of average points on the creep curves for all levels of T. The following values were found for the parameters: $a$ = 0.78·10$^{-4}$ mm$^2$/kgf, b = 1.09·10$^{-4}$ mm$^2$/kgf, $\tau_1$ = 0.55·10$^{-1}$ h, $\tau_2$ = 0.4·10$^2$ h,

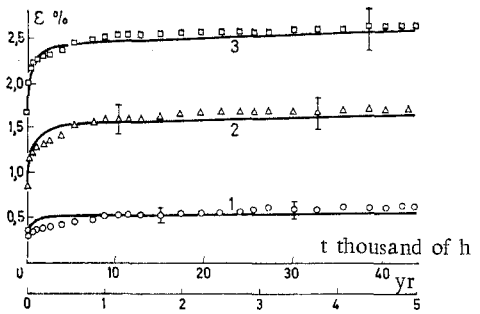


Fig. 5

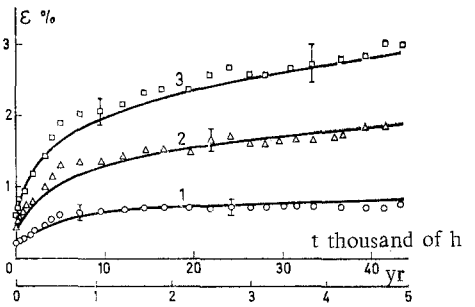


Fig. 6

Fig. 5. Long-term creep of organic fibers under stresses $\sigma$ = 33 (1), 100 (2), and 165 kgf/mm$^2$ (3). Points indicate control experiments; lines denote prediction.

Fig. 6. Long-term creep of solidified binder under stresses $\sigma$ = 0.68 (1), 1.36 (2), and 2.04 kgf/mm$^2$ (3). Points indicate control experiments; lines denote prediction.

$\tau_3 = 1.3 \cdot 10^3$ h, and $\tau_4 = 7.67 \cdot 10^4$ h for the fibers, and $a = 31.9 \cdot 10^{-4}$ mm$^2$/kgf, $b = 149 \cdot 10^{-4}$ mm$^2$/kgf, $\tau_1 = 4.5 \cdot 10^3$ h, and $\tau_2 = \tau_3 = 5.0 \cdot 10^4$ h.

The accuracy of the description of the experimental curves can be judged from Figs. 3 and 4 in which average experimental yield curves for the fiber and binder at different temperatures and curves computed from (10) using the above-cited characteristics are presented. The error of approximation does not exceed the confidence interval of the average experimental points; the relative mean-square error, which characterizes the descrepancy between the computed data and the average experimental data, is 3.7% and 4.8% for the creep curve of the fiber and binder, respectively. Thus, the initial creep curves for the fiber and binder in the temperature region investigated are described completely satisfactorily with allowance for the corresponding $a_T$ functions. The characteristics determined in this case make it possible to describe the creep at the base temperature in a time interval exceeding the duration of the accelerated tests by several orders of magnitude. What is the validity of this prediction? This question is answered by comparing the results of prediction with long-term control tests.

Experimental curves of the 5-yr creep of the fiber and binder specimens, which were averaged from five concurrent tests, are presented in Figs. 5 and 6. The stress levels of 33, 100, and 165 kgf/mm$^2$ used for the fiber were, respectively, 0.1, 0.3, and 0.5 of the ultimate short-term strength; the stresses of 0.68, 1.36, and 2.04 kgf/mm$^2$ used for the binder were, respectively, 0.1, 0.2, and 0.3 of R. Random temperature fluctuations during long-term testing did not extend beyond the 17-22°C interval, and relative humidity ranged from 50-70%. The certain nonmonotonic character of the variation in the experimental creep curves was apparently caused by instability of the temperature-humidity conditions in the rooms where the long-term tests were conducted.

A significant difference between the character of the long-term creep curves for the binder and fibers follows from Figs. 5 and 6. In contrast to the binder, the basic part of the creep strains in the fiber is realized over the course of the first three to five months of testing; thereafter, the creep rate of the fiber diminishes appreciably; strictly speaking, however, it cannot be considered zero even after five years of testing. Also shown in Figs. 5 and 6 are creep curves predicted from the above-cited characteristics obtained from accelerated temperature tests. The maximum deviation of these curves from the average experimental points was 25%; the relative mean-square error of the prediction does not exceed the confidence intervals of the experimental curves. Thus, the fact that the temperature tests for short-term creep made it possible to predict the long-term strength of fiber and binder completely satisfactorily can be considered established.

Let us now assess the possibility of predicting the long-term creep of a plastic with a given reinforcing factor from the properties of the components (fiber and binder) as determined from accelerated tests. The computations were performed on an ES-1022 computer in accordance with relation (9) for a unidirectional reinforced organoplastic with a volumetric fiber content of 0.65. Control creep tests of this material were carried out over the course

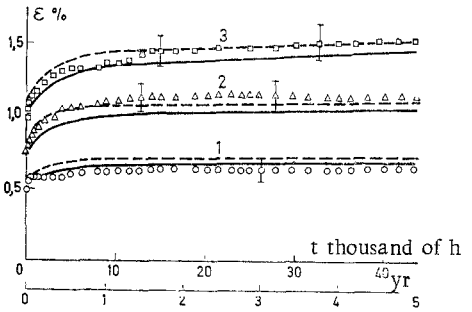


Fig. 7

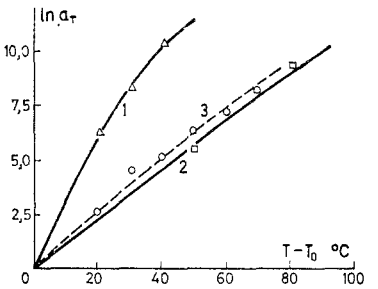


Fig. 8

Fig. 7. Long-term creep of unidirectional reinforced organoplastic under tension in direction of reinforcement; $\sigma$ = 30 (1), 45 (2), and 60 kgf/mm$^2$ (3). Points indicate control experiments; lines denote prediction from accelerated tests of fiber and binder and subsequent computation of creep of organoplastic (---) and from accelerated tests of organoplastic specimens (——).

Fig. 8. Temperature–shear functions for binder (1), organic fiber (2), and organoplastic (3) at base temperature $T_0$ = 20°C.

of five years under tension in the direction of the reinforcement at stresses of 30, 45, and 60 kgf/mm$^2$; this was, respectively, 0.2, 0.3, and 0.4 of the ultimate short-term strength. The temperature–humidity conditions of the tests were similar to those of the long-term tests of the fiber and binder specimens. The results of prediction and control tests of the organoplastic are presented in Fig. 7, from which it is apparent that the creep curves of the plastic as predicted from the properties of the components correspond wholly satisfactorily with the averaged experimental curve; the relative mean-square deviation of the curves is 8.75%. Also shown in Fig. 7 are creep curves predicted from the results of accelerated temperature tests of organoplastic specimens.

We tested the composite for short-term (up to 5 h) creep at seven temperature levels in the 20-90°C range; the resultant data were analyzed in accordance with the above-described scheme (for the fiber and binder). In describing the family of I(ln t, T) curves of the composite, there was no clear-cut nonobservance of the temperature–time analogy. The temperature–shear function derived from the composite is shown in Fig. 8, in which $a_T$ functions for the binder and fiber are also presented for comparison.

At first glance, the conclusion concerning the thermorheologically simple behavior of the composite contradicts the considerations made in the first part of this paper. In effect, the temperature–shear functions at $T_0$ = 20°C for the fiber and binder differ significantly: at T = 60°C, for example, their values differ by two orders of magnitude ($a_{T\alpha} = 1.22 \cdot 10^2$, and $a_{Tm} = 2.97 \cdot 10^4$). As has already been noted, however, observance of the temperature–time analogy for the fibrous composite is determined not only by the difference between $a_{T\alpha}$ and $a_{Tm}$, but also to a large degree by the relationship between the yield values of the structural components and the magnitude of the reinforcing factor. To confirm this, we computed the yield of a composite with different values of $\mu$ (in the 0.1-0.7 range) from relationship (9) for several temperature levels. To evaluate the effect of the difference between $a_{T\alpha}$ and $a_{Tm}$, the computations were performed for two levels: actual (differing) functions of $a_{Tm}$ and $a_{T\alpha}$ were assigned in the first case (see Fig. 8), and $a_{Tm}$ values equal to $a_{T\alpha}$ were adopted in the second. It was found that the isochronic yield curves of a composite with a volumetric fiber content of from 0.3 to 0.7, which were computed for the conditions, differed one from the other by less than 2% in the temperature range from 20 to 90°C; it was also found that only under smaller values of $\mu$ did this discrepancy begin to increase markedly. In describing the family of I(t, T) curves for organoplastic with $\mu$ = 0.65, consequently, no nonobservance of the temperature–time analogy could be determined, since the scatter of experimental data in the creep tests, as a rule, was appreciably greater. The temperature–shear function derived from testing the organoplastic was therefore close to the $a_{T\alpha}$ function (see Fig. 8). Thus, the question concerning the thermorheological complex behavior of the organoplastic under investigation may, of course, be of theoretical interest in virtually the entire critical range of the reinforcing factor; for practical problems involving prediction, however, the

assumption concerning observance of the temperature–time analogy is totally acceptable for the composite. As is apparent from Fig. 7, the accuracy of the prediction in this case is no worse than the prediction from accelerated tests of the structural components. It is natural that the results of these accelerated tests be used to predict the creep of just the composite tested for a specific reinforcing factor. Where necessary, preliminary prediction of the creep functions of the fiber and binder and subsequent computation of the long-term creep of a composite with a different volumetric fiber content is preferable to varying $\mu$.

## LITERATURE CITED


1. V. V. Kovriga, E. S. Osipova, I. I. Farberova, and K. Ya. Artanova, "Temperature–time superposition as applied to the relaxation properties of fiberglass and its binder," Mekh. Polim., No. 2, 360-363 (1972).
2. V. S. Ekel'chik, S. N. Kostritskii, and M. Z. Tsirkin, "Temperature–time relationship for the strength and deformability of fiberglasses in the transversal direction," in: First All-Union Conference on Composition Polymer Materials and Their Application in the National Economy. Theses of Papers [in Russian], Vol. 2, Tashkent (1980), p. 51.
3. R. D. Maksimov, Ch. L. Daugste, and E. A. Sokolov, "Characteristic features of the observance of the temperature–time analogy during the physically nonlinear creep of a polymer material," Mekh. Polim., No. 3, 415-426 (1974).
4. Yu. S. Urzhumtsev and R. D. Maksimov, Predicting the Deformability of Polymer Materials [in Russian], Riga (1975).
5. Yu. S. Pervushin, V. P. Pavlov, and V. V. Zainullin, "On the application of the temperature–time analogy to computation of creep strains in fiberglasses in a nonsteady temperature field," Probl. Prochn., No. 7, 27-29 (1976).
6. R. Sheperi, "Viscoelastic behavior of composition materials," in: Composition Materials. Vol. 2. Mechanics of Composition Materials [in Russian], Moscow (1978), pp. 102-195.
7. W. J. Griffith, D. H. Morse, and H. F. Brinson, "Accelerated characterization of graphite/epoxy composites," Advances in Composite Materials. Proceedings of the Third International Conference on Composition Materials, Vol. 1, Paris (1980), pp. 461-471.
8. H. T. Hahn and T. T. Chiao, "Long-term behavior of composite materials," Advances in Composite Materials. Proceedings of the Third International Conference on Composition Materials, Vol. 1, Paris (1980), pp. 584-596.
9. V. V. Moskvitin, Strength of Viscoelastic Materials [in Russian], Moscow (1972).
10. Yu. N. Rabotnov, Elements of the Hereditary Mechanics of Solids [in Russian], Moscow (1976).
11. A. F. Kregers, "An algorithm for determination of the parameters of the resolvent (kernel) of one-dimensional linear viscoelasticity from given parameters of the kernel (resolvent) represented by the sum of the exponents," Algoritmy Programmy, No. 1, 27 (1975).
12. E. A. Sokolov and R. D. Maksimov, "Possibility of predicting the creep of a polymer-fiber reinforced plastic from component properties," Mekh. Polim., No. 6, 1005-1012 (1978).
13. Yu. V. Suvorova, I. V. Viktorova, and G. P. Mashinskaya, "Long-term strength and failure of organoplastics," Mekh. Kompozitn. Mater., No. 6, 1010-1013 (1980).
14. G. M. Gunyaev, Structure and Properties of Fibrous Polymer Composites [in Russian], Moscow (1981).
15. V. N. Efimova and R. D. Maksimov, "Comparative analysis of the temperature–time relationship between the deformation properties of polyvinyl chloride in the linear and nonlinear regions of viscoelasticity," Mekh. Polim., No. 2, 213-219 (1977).
16. É. Z. Plume, "An algorithm for confirming the observance of the temperature–time analogy in temperature–time relationships of the deformation and strength properties of polymers, Algoritmy Programmy, No. 2, 34 (1978).
17. A. F. Kregers, "An algorithm for searching the minimum of a multiple-variable function by the descent method," Algoritmy Programmy, No. 2, 9 (1974).